Biochimica et Biophysica Acta, 1070 (1991) 265–273

BBAMEM 75443

Low levels of the pesticide, δ-hexachlorocyclohexane, lyses human erythrocytes and alters the organization of membrane lipids and proteins as revealed by Raman spectroscopy

Surendra P. Verma [1] and Arun Singhal [2]

[1] *Department of Community Health, Tufts University School of Medicine, Boston, MA (U.S.A.)* and [2] *Department of Radiation Oncology, Medical College of Virginia, Richmond, VA (U.S.A.)*

Received 1 May 1991)
(Revised manuscript received 8 July 1991)

Key words: Pesticide; Hexachlorocyclohexane; Erythrocyte membrane; Raman spectroscopy; Thermal transition; Protein structure

We studied the nature of the interaction of δ-hexachlorocyclohexane (δ-HCCH), a pesticide having a stereoisomeric structure similar to inositol, with red blood cells. Cell survival data, measured as percent of hemoglobin released by δ-HCCH, show that the cell lysis increases with post exposure time. δ-HCCH at 55–60 μg/ml causes about 70% cell lysis after 24 h of exposure. The nature of interaction of δ-HCCH with membrane components was evaluated by studying the thermotropic transitions and protein structure of ghosts using Raman spectroscopy. Control ghosts show transitions with onset/completion temperatures 30 °C/38 °C (high temperature transition) and 3 °C/10 °C (middle temperature transition) when monitored by the I_{2935}/I_{2850} ratio. The interaction of δ-HCCH drastically broadens the high temperature transition and shifts it to the temperature range of 10–29 °C. The plots of ($I_{2880\text{-}90}/I_{2850}$) vs. temperature show two transitions for control ghosts, one extending from −10 °C to 3 °C (lower temperature transition) and the other from about 7 °C to about 15 °C (middle temperature transition). Ghosts lysed with δ-HCCH shows only a single and a very broad transition in the range of about −3 °C to about 15 °C. These changes in the thermal transition properties suggest that δ-HCCH alters lipid and lipid-protein phases of erythrocyte membranes. The comparison of Raman spectra in the amide I and III regions of erythrocyte ghosts and purified band 3 with several amidated compounds reveals that cytoskeleton proteins contain highly amidated residues (probably glutamine and asparagine). The interaction of δ-HCCH with erythrocytes drastically alters the environment of these amidated residues indicating the involvement of cytoskeleton proteins. We conclude that the interaction of δ-HCCH with red blood cells disrupt membrane structure and change the environment of cytoskeleton proteins that could cause cell lysis.

Introduction

Hexachlorocyclohexanes (HCCH) are available in four stable isomers known as α, β, γ and δ, depending on the number of axial and equatorial chlorine atoms in the molecule [1]. γ-HCCH, used as a pesticide called lindane, acts as a convulsant and evokes hyperexcitability and tremors in insects [2]. The exposure of these chlorinated pesticides to humans could cause diverse health effects. The molecular mechanisms of the interaction of these chemicals with cells have not been fully understood. Several studies suggest that the site of action of these molecules is in the membranes [3,4]. Chlorinated pesticides have been shown to change the activities of muscle plasma membrane enzymes [5] and (Ca^{2+} + Mg^{2+})-ATPase from sarcoplasmic reticulum [6]. These pesticides also alter the γ-aminobutyric-dependent chloride flux into mouse brain vesicles [7] as well as permeabilities of Ca^{2+} [8] and Na^+ and K^+ ions [9].

Studies on the HCCH–membrane interaction are also interesting due to their configurational similarity with inositols. Inositol triphosphate, produced as a result of agonist-induced cleavage of phosphatidyl inositol, acts as a second messenger to mobilize calcium

Abbreviation: HCCH, hexachlorocyclohexane.

Correspondence: S.P. Verma, Department of Community Health, Tufts University School of Medicine, 136 Harrison Avenue, Boston, MA 02111, U.S.A.

from intracellular stores [10]. Both γ- and δ-HCCHs have been shown to inhibit the synthesis of phosphatidyl inositol in several intact cells [11–13]. The δ-HCCH isomer at 4 mM concentrations also inhibits the activities of CDP-choline: 1,2-diacyl-*sn*-glycerol cholinephosphotransferase (PC synthase) in mouse pancreas microsomes, membrane-associated 1,2-diacylglycerol kinase in mouse brain microsomes, Na^+,K^+-ATPase in mouse brain microsomes and human erythrocyte ghosts [14]. The precise mechanism for the δ-HCCH-induced inhibition of activities of membrane-associated enzymes is not clear. It has been proposed that the enzyme inhibition could result directly from the insertion of γ- or δ-HCCH into the hydrophobic domains of enzymes or indirectly via affecting the enzyme-associated annular lipids rather than from a general perturbation of membrane bilayer structure [14].

α-, γ- and δ-HCCHs have been reported to act as a potent stimuli for the production of superoxide anion and the release of calcium in human polymorphonuclear leukocytes [15]. The order of toxicity of HCCH isomers as determined in the above paper is ($\gamma > \alpha > \delta > \beta$) which is somewhat dissimilar to the toxicity order ($\delta > \gamma > \alpha > \beta$) reported in Ref. 14. Kuhns et al. [15] argue that the involvement of membrane perturbation or altered membrane fluidity by HCCH isomers, as determined by using a lipid analogue fluorescence probe [16], is unlikely to account for their toxicity. It is possible that the fluorescence probe used by these researchers could have itself fluidized lipid bilayers and that the further insertion of HCCHs into these fluid lipid bilayers would not change the fluorescing properties of the probe. However, using 1,6-diphenyl-1,3,5-hexatriene (DPH) as a fluorescence probe, lindane has been shown to disorganize the gel phase of phospholipid liposomes [17]. We have also reported recently that both δ- and γ-HCCHs drastically lower the thermal transition temperatures of phospholipids [18]. DDT [19], herbicides and several other phenylamides [20] have also been shown to broaden and shift the phase transition temperature of phospholipid bilayers. In general, membranes are implicated as the site of action for HCCHs but the molecular nature of the interaction is yet unclear.

In this communication, we report that δ-HCCH lyses human erythrocytes at low concentrations. Lysing could result from the interaction of δ-HCCH with membrane lipids that in turn may affect the conformation of the cytoskeleton proteins.

Materials and Methods

Materials. δ-HCCH and various amino acids were obtained from Sigma Chemical Co. (St. Louis, MO). Other chemicals used to prepare buffers were reagent grade.

Erythrocytes. Erythrocytes were isolated from freshly drawn blood from human volunteers in heparin (10 U/ml) and were washed three times with PBS using a table top centrifuge to remove plasma and leukocytes. The washed erythrocytes (about 10^8 cells) were used for survival experiments as well as for the preparation of erythrocyte ghosts.

Survival. The cell survival experiments were carried out as follows: Stock solution of δ-HCCH was made in dimethyl sulfoxide (DMSO). Various concentrations of δ-HCCH were added to washed erythrocytes (about 10^8 cells suspended in PBS containing glucose (1 mg/ml). The final concentration of DMSO did not exceed 0.5% (v/v). Control erythrocytes were treated identically with the solvent DMSO without δ-HCCH. All samples were incubated at 37 °C. At specified time points, cells were centrifuged and lysis of erythrocytes by δ-HCCH was determined by measuring optical density of supernatant hemoglobin at 452 nm. Optical density for 100% lysis was obtained by lysing the equal volume of erythrocytes in water. The percent cell survival was calculated by using the following equation:

$$100 - \frac{\text{O.D. of } \delta\text{-HCCH lysed cells}}{\text{O.D. of 100\% lysed cells}} \times 100$$

Erythrocyte ghosts for Raman spectroscopy. About 10^8 cells in PBS (pH 7.4) were mixed with 55 μg/ml of δ-HCCH followed by incubation at 37 °C for 24 h. Under these conditions, about 70% of the cells were lysed. The unlysed cells were removed by centrifugation. Erythrocyte ghosts were centrifuged at 15000 rpm for 30 min. The pelleted ghosts were washed three times with PBS. Control ghosts were prepared by lysing erythrocytes with 5 mM phosphate buffer (pH 7.4) containing 0.5% v/v DMSO. The washed membranes were concentrated by a Beckman airfuge (100000 rpm for 15 min). The tightly packed pellets were transferred to Kimax capillaries for Raman spectroscopy.

Total lipids of ghosts were isolated by chloroform/methanol (2:1; v/v) mixture under nitrogen. Lipid extracts were washed, dried under vacuum for 2 h and were suspended in 5 mM phosphate (pH 7.4). The hydrated total lipids were placed in a water bath at 37 °C and were periodically agitated by vortex to prepare liposomes.

Raman spectroscopy. Raman spectra were recorded using a Triplemate spectrometer (Model 1877, Spex Industries, Edison, N.J.) and an Optical Spectrometric Multichannel Analysis (OSMA) system (Princeton Instruments, Trenton, N.J.). An IRY 700 (visible/blue) detector head, cooled to −20 °C and a ST120 controller, interfaced to an IBM compatible AT computer

(Zenith 386) were used to detect and process the Raman spectra. Samples sealed in Kimax capillaries were excited by an Ar ion laser (Spectra Physics, Model 164) tuned at 514.5 nm (power 300 mW). Sample temperature was controlled by a flow of temperature regulated (measured by a thermistor) nitrogen gas in a Harney-Miller cell. The exposure time was 6.667 s per exposure and a minimum of 100 spectra were stored and averaged. Averaged spectra were processed as mentioned below, calibrated and finally plotted using a Hewlett Packard plotter (Model Color Pro). Indene was used for frequency calibration in the 1100–1800 cm^{-1} region. Stearic (room temperature) and linolenic acids (−20 °C) were used to calibrate the C-H stretching region.

Analysis of Raman spectra. The spectral contributions of total lipids and water were subtracted from the spectra of erythrocyte ghosts as in Refs. 21 and 22). The concentration of water in ghosts was estimated from the water band around 3400 cm^{-1}. The normalized water spectrum in the amide I region was subtracted from spectra of ghosts and liposomes prepared from total lipid extracts. The water subtracted spectra of liposomes and ghosts were normalized to match the counts at 1746 cm^{-1} (Fig. 2). The normalized spectrum of liposomes of total lipids were then subtracted from the spectrum of normalized ghosts. The final spectra presented in Figs. 5 and 7 were smoothed (9-point smoothing).

Results

Cell survival

The lysis of red blood cells, represented as surviving fraction, as a function of δ-HCCH concentration at 3, 12 and 24 h post treatment time are shown in Fig. 1. The lysis of red blood cells by δ-HCCH is not instantaneous. It depends on post exposure time. After 3 h, the lysis is negligible but increases with time. To check whether the lysate of red blood cell could cause time-dependent lysis, we added cell free lysate in saline to control cells and did not observe any appreciable lysis. The lysis of red blood cells could thus be due to the slow diffusion of δ-HCCH into the cells.

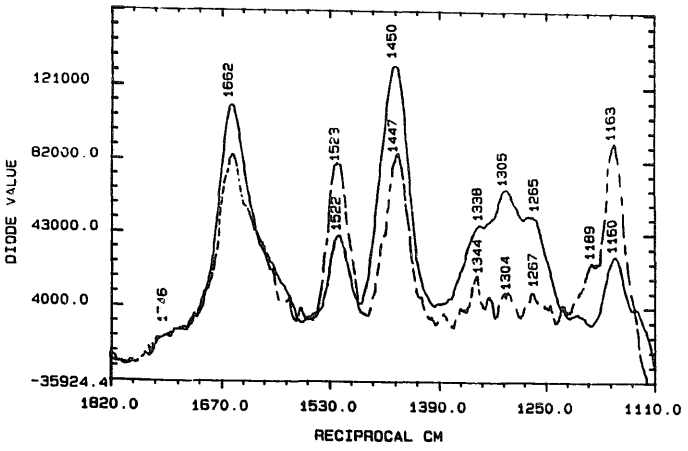

Fig. 2. Raman spectra of control erythrocyte ghosts (solid line) and liposomes prepared from total lipid extracts of ghost membranes (broken lines). Spectra recording conditions: incident radiation, 514.5 nm, 300 mW power; exposure time, 6.667 s per exposure; total scans, 100; smoothing 9 points.

C-H stretching and thermotropic properties

Raman spectra of control and δ-HCCH lysed erythrocyte ghosts were recorded in the C-H stretching region (2800–3000 cm^{-1}) as a function of temperature (−10 °C to 46 °C). Three strong features occur at 2850, 2880-90 and 2935 cm^{-1} [23]. We used plots of (I_{2935}/I_{2850}) vs. temperature (Fig. 3) and ($I_{2980\text{-}90}/I_{2850}$) vs. temperature (Fig. 4) for the estimation of thermotropic properties of lipid and lipid/protein phases [23]. The temperatures reported in Figs. 3 and 4 are uncorrected. The heating caused by the laser light is in

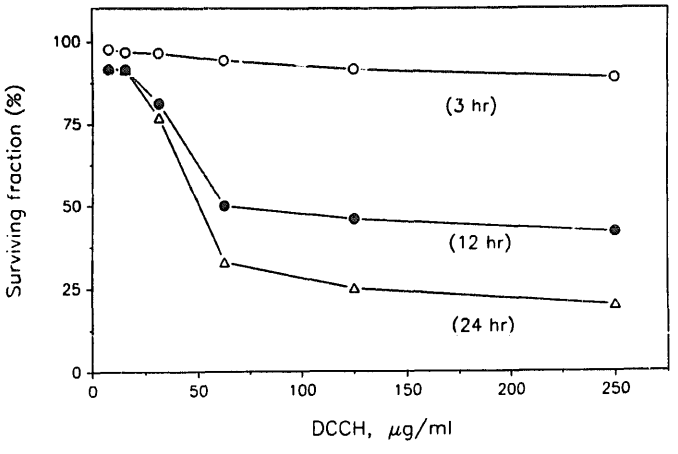

Fig. 1. Percent survival of erythrocytes plotted as a function of the concentration of δ-hexachlorocyclohexane. Percent survival was calculated at 3, 12 and 24 h post treatment.

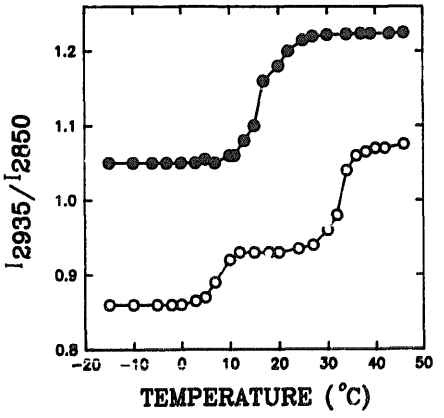

Fig. 3. Plots of the intensity ratio (I_{2935}/I_{2850}) vs. temperature for control ghosts (open circles) and ghosts prepared from δ-hexachlorocyclohexane-treated (55 μg/ml for 24 h) erythrocytes (solid circles). Spectral contributions of water was subtracted from the C-H stretching spectra of ghosts. Recording conditions are given in Fig. 2.

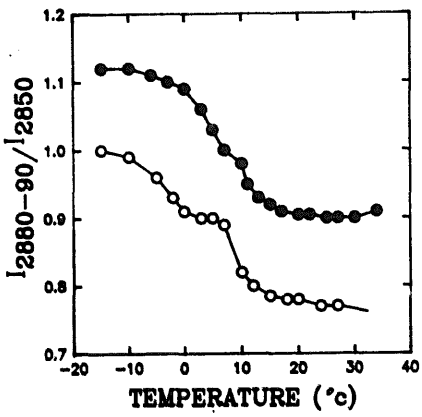

Fig. 4. Plots of the intensity ratio ($I_{2880\text{-}90}/I_{2850}$) vs. temperature for control ghosts (open circles) and ghosts prepared from δ-hexachlorocyclohexane-treated (55 μg/ml for 24 h) erythrocytes (solid circles). Spectra recording conditions are given in Fig. 2.

the range of 2–3 °C as determined by the melting points of authentic fatty acids.

In Fig. 3, (open circles), the ratio (I_{2935}/I_{2850}) shows two transitions for control ghosts. One in the temperature range of about 30 °C to about 38 °C (midpoint about 33 °C, high temperature transition) and another in the temperature range of about 3 °C to 10 °C (middle temperature transition, midpoint about 6 °C), manifested by a smaller change in the ratio.

δ-HCCH lysed ghosts show several drastic changes in the transition properties as measured by the ratio (I_{2935}/I_{2850}) (Fig. 3, solid circles). (1) The high temperature transition (midpoint about 33 °C) considerably broadens and shifts to the lower temperature range extending from about 10 °C to about 29 °C (midpoint about 18 °C). (2) The values of the ratio (I_{2935}/I_{2850}) are always higher at each data point in comparison to the values of the control samples. (3) The ratio (I_{2935}/I_{2850}) does not show any transition in the middle or lower temperature range.

Thermotropic properties of both control and δ-HCCH lysed ghosts, as monitored by the ratio ($I_{2880\text{-}90}/I_{2850}$), are shown in Fig. 4. Control ghosts show two transitions (Fig. 4, open circles). The lower temperature transition extends from about −10 °C to about 3 °C (midpoint about −5 °C) and the range of the middle temperature transition is about from 7 °C to about 15 °C (midpoint about 9 °C). These thermal transition ranges are very close to those reported by us previously [23]. Slight changes could be attributed to the formation of small vesicles by high speed centrifugation of ghosts in the present studies.

Thermal transitions of δ-HCCH lysed ghosts as evaluated from the ($I_{2880\text{-}90}/I_{2850}$) vs. temperature plot (Fig. 4, solid circles) also reveal drastic changes. This plot shows only a single and a very broad transition in the temperature range of −3 °C to about 15 °C.

Raman spectra in the 1100–1750 cm^{-1} region

Representative Raman spectra of control (thin line spectrum) and δ-HCCH lysed ghosts (thick line spectrum) in the 1100–1750 cm^{-1} region are shown in Fig. 5. Spectral contributions of water and total lipids have been subtracted from these spectra as mentioned in Methods and shown in Fig. 2. Most of the features shown in these spectra (Fig. 5) are thus contributed by proteins except two resonance Raman bands around 1522 and 1160 cm^{-1}, assigned to carotenoids. A small amount of carotenoids might be associated with integral membrane proteins and could not be extracted in total lipids by chloroform:methanol mixture [24]. The spectrum of control ghosts is virtually similar to those reported previously [25,26]. Band assignments for proteins are taken from [27,28]. The conformational-sensitive features of proteins occur in the amide I and III regions. Characteristic vibrations of side chains of amino acid residues also appear in these regions.

Control ghosts (Fig. 5, thin line spectrum) yield two strong amide I features, a band at 1660 cm^{-1} and a shoulder around 1653 cm^{-1} (these features are not marked in the figure for the sake of clarity), assigned to unordered and α-helical configuration, respectively. There are also two somewhat weaker shoulders around 1615 and 1598 cm^{-1} which are generally assigned to ring vibrations of tyrosine (Tyr) and phenylalanine (Phe) residues [26,27]. As we shall see latter that glutamine, asparagine residues and several other amidated compounds also yield environment-sensitive strong features in the 1600 ± 20 cm^{-1} region [29].

The amide III region (1200–1350 cm^{-1}) yields multiple features that are comparatively more sensitive to protein conformation. Major bands peak at 1265, 1307,

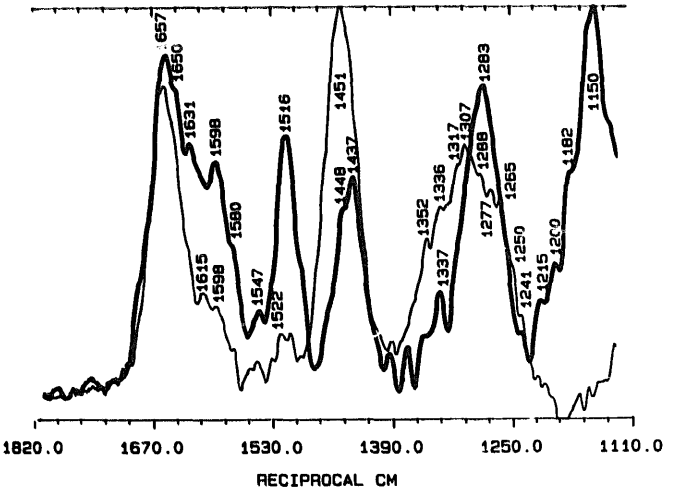

Fig. 5. Raman spectra of control erythrocyte ghosts (thin-line spectrum) and ghosts prepared from δ-hexachlorocyclohexane-treated (55 μg/ml for 24 h) erythrocytes (thick-line spectrum), showing the 1100–1750 cm^{-1} region. Spectra recording conditions are given in Fig. 2. Spectral contributions of water and total lipids of ghosts have been subtracted from these spectra using the procedure outlined in Methods and Fig. 2.

1336 and 1352 cm^{-1} while weak shoulders appear around 1241, 1250, 1277, 1288 and 1317 cm^{-1}. In the literature, the 1265 and 1307 cm^{-1} features are assigned to amide III band of α-helical segments of proteins and CH_2 twist of long acyl chains, respectively [25,26]. Since we subtracted the spectral contribution of total lipids from the present spectrum and since the total lipid extracts do not show a major band at 1307 cm^{-1} (Fig. 2), we assign this feature also to amide III band of α-helical segments of proteins. However, the 1307 cm^{-1} feature also may represent vibrations of secondary amides [30] or of amidated proteins [29] as discussed latter. The C-H deformation band occurs at 1451 cm^{-1}.

δ-HCCH lysed ghosts show major spectral changes in the 1500–1700 cm^{-1} and 1200–1350 cm^{-1} regions (Fig. 5, thick line spectrum). The concentration of δ-HCCH is very low and does not show strong band/s in these regions [18]. We assign the observed spectral changes to alterations in the conformation of membrane proteins. A strong peak appears at 1657 cm^{-1} together with strong shoulders around 1650 and 1668 cm^{-1} which are assigned to α-helical (1650 and 1657 cm^{-1}) and β sheets (1668 cm^{-1}) [27,28]. The most notable difference seen in these spectra is that the intensities of bands in the region from about 1631 to about 1580 cm^{-1} are enhanced in the δ-HCCH lysed ghosts. Similarly in the amide III region, the intensities of the 1307, 1317, 1336 and 1352 cm^{-1} features are either considerably reduced or these bands are shifted towards the lower frequencies while the intensity of the 1283 cm^{-1} band is dramatically increased. Because of the enhancement of the 1283 cm^{-1} feature, other bands or shoulders in this region are overshadowed or less resolved.

Raman spectra of some relevant amino acids and amidated compounds

Amidated compounds, some amino acids other than aromatic amino acids and secondary amides show strong bands in the 1600 and 1300 ± 20 cm^{-1} region [28,30]. Therefore, the appearance of enhanced bands/shoulders around 1600 ± 20 cm^{-1} and 1300 cm^{-1} in the Raman spectra of both control and δ-HCCH lysed erythrocyte ghosts also may indicate the presence of amidated proteins. Glutamate and aspartate residues of membrane proteins are the most likely candidates for amidation. We have therefore recorded Raman spectra of some amidated compounds and authentic amino acids. Several of our spectra are given in Fig. 6.

Asparagine, glutamine and tyrosine show bands at 1618, 1620 and 1621 cm^{-1}, respectively in the amide I region. The feature at 1615 cm^{-1} in control ghosts could therefore arise from aspartate and glutamate as well as from tyrosine residues. Both asparagine (solid)

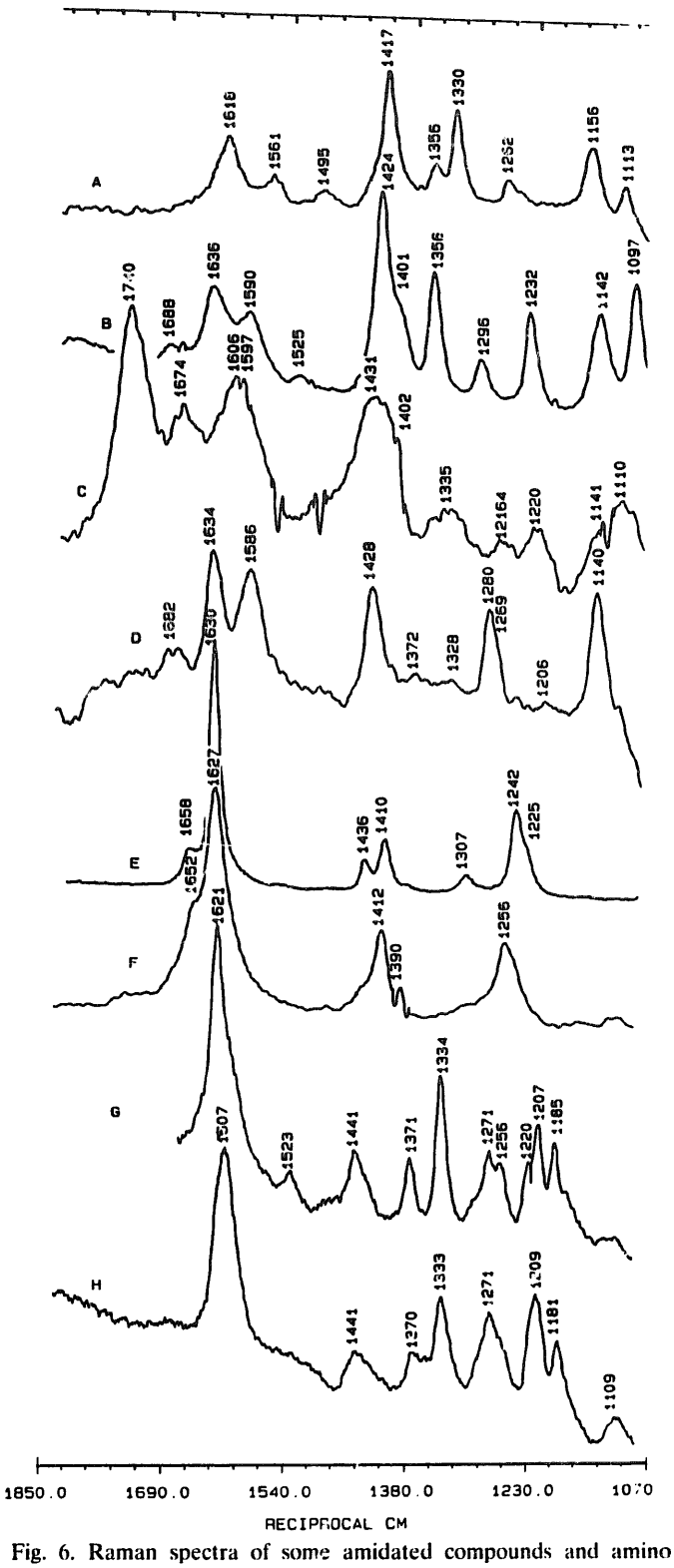

Fig. 6. Raman spectra of some amidated compounds and amino acids. Spectral contribution of water (whenever used) has not been subtracted from these spectra. A, Asparagine (solid); B, asparagine (solid and wet with 0.1 M KCl); C, asparagine (solution in conc. HCl); D, acrylamide (solid); E, bisacrylamide (solid); F, bisacrylamide (acidic solution); G, tyrosine (solid); H, tyrosine (basic solution).

and tyrosine (solid yield strong bands at 1330 and 1334 cm^{-1}, respectively (Fig. 6 G, H). The asparagine bands shift when recorded in 0.1 M KCl. The 1618 cm^{-1}

band of asparagine splits into 1636 and 1590 cm^{-1}, and the 1356 cm^{-1} band becomes strong. All bands below 1330 cm^{-1} shift to lower frequencies (Fig. 6B). Asparagine, dissolved in concentrated HCl, shows a strong band at 1740 (carbonyl frequency). Bands in the Amide I region appear at 1674, 1606 and 1597 cm^{-1} and intensities of all the amide III bands reduced (Fig. 6C). Asparagine, in NaOH solution, shows strong bands at 1664 and 1604 cm^{-1} in the amide I region and somewhat weaker bands at 1354, 1323 and 1311 cm^{-1} and a weak shoulder around 1261 cm^{-1} (spectrum not shown) in the amide III region.

Variation in the environment (e.g., solution in NaOH, phosphotyrosine etc.) of tyrosine shows a shift in the frequency of ring vibration from 1620 to 1607 cm^{-1} (Fig. 6G, H). However, Raman features of tyrosine in the amide III region do not shift drastically as seen in asparagine. Raman spectra of phosphotyrosine (Sigma) shows a strong ring vibration at 1616 cm^{-1} in the amide I region and two new strong bands at 1241 and 1214 cm^{-1}, assigned to phosphate group, in the amide III region (spectrum not shown). Raman spectrum of phosphotyrosine solubilized in NaOH, shows a shift in the ring vibration to 1607 cm^{-1} while the phosphate vibrations are weaker and shifted to 1229 cm^{-1}. Histidine yields two strong bands at 1314 and 1268 cm^{-1} in the amide III region (assigned to two tautomeric forms) [27] and weaker bands at 1564 and 1541 cm^{-1} in the amide II region.

Raman spectra of some other amidated compounds also show strong bands in the amide I and III regions. For example, acrylamide (solid) shows bands at 1634, 1586 cm^{-1} in the 1600 cm^{-1} region and a strong band at 1280 cm^{-1} and a weak shoulder around 1269 cm^{-1} in the amide III region (Fig. 6D). Bisacrylamide (solid) shows bands at 1658 cm^{-1} (strong) and 1630 cm^{-1} (very strong) in the amide I region and two bands at 1242 cm^{-1} (strong) and 1307 cm^{-1} (weak) in the amide III region (Fig. 6E). The acidic solution of Bisacrylamide yields bands at 1627 cm^{-1} (shifted downwards by 3 cm^{-1}) and 1256 cm^{-1} (shifted upwards by 11 cm^{-1}) (Fig. 6F). The secondary amides of the type *N*-methyl- or *N*-ethylacetamide also show strong bands at 1300 and 1295 cm^{-1}, respectively [30].

Discussion

A wealth of published information has shown that HCCH pesticides can disrupt the structure of lipid bilayers and can interact with and inhibit the activities of several membrane-associated enzymes. Since no specific mechanism(s) for the uptake of these molecules by erythrocytes or by other cell systems have been proposed so far, we therefore assume that these molecules partition into red blood cells according to their lipophilic nature. δ-HCCH would partition into the hydrophobic domains of lipids and also could accumulate in the hydrophobic sites of membrane proteins.

The survival curves show that δ-HCCH is highly disruptive to erythrocyte membranes after 12–24 h of incubation. The breakdown of membranes is both time and concentration dependent. About 50% of the cells are broken in the presence of approx. 60 μg/ml of δ-HCCH at 12 h post treatment. After 24 h, about 75% cell are lysed. The cell lysis could occur due to the insertion of δ-HCCH into either the lipid bilayer or in the hydrophobic sites of proteins. Both processes could result into breaking the membranous structure and leaking of hemoglobin. Since the effect of δ-HCCH is slow, this may suggest that hemolysis could be a secondary effect.

Our Raman data show that the interaction of δ-HCCH with erythrocyte membranes alters both lipid and protein organization. Membrane disruption could make red cells leaky. However, in a natural membrane system, it is difficult to establish precisely that whether the disordering of lipid bilayer by the pesticide has led to the altered structure of proteins or vice versa.

The properties of thermal transition are sensitive physical parameters for determining the ordering and disordering behavior of lipids in bilayer membranes. The spectral properties of the C-H stretching region bands of membranes have been successfully used to evaluate the physical state of lipids and proteins [23]. Our data showing changes in the transition properties suggest that δ-HCCH induces reorganization of remixing of acyl chains. This is possible since acyl chains must reorganize to cope with the insertion of nonplanar and 'chair' configuration δ-HCCH molecules.

Plots of the ratio (I_{2935}/I_{2850}) vs. temperature show a high temperature transition in the range of 30 °C to 38 °C for normal ghosts but not for liposomes prepared from total lipid extracts. This transition perhaps reveals dominantly the physical state of interfaces between hydrocarbon residues of membrane proteins and lipids [31–33]. The 2935 cm^{-1} feature, a methyl residue stretching vibration, is contributed by both lipids and proteins. Its intensity depends on the physical states of both lipids and proteins. In biological membranes, proteins have a higher mass in comparison to lipids (approximately 3:2; protein/lipid mass ratio) and hence the spectral contribution of their methyl residues towards the intensity of 2935 cm^{-1} band is also higher. The intensity of 2935 cm^{-1} band of erythrocyte ghosts has been found sensitive to the folding defects of proteins created by higher temperature and low pH [31] and on the imposition of transmembrane potential [34]. The state of proteins, represented by the pH dependent shift in the thermal transitions of erythrocyte membranes [31], could be similar to the pH-dependent protein aggregation process reported by Pinto

da Silva [35]. The (I_{2935}/I_{2850}) vs. temperature plot of egg lecithin-RNAse liposomes have shown a transition range (midpoint about 35 °C) [36] which corresponds in position and width to the transition detected by differential thermal calorimetry [37]. Egg lecithin alone shows a transition at −6 °C and insertion of protein (band 3) decreases the phospholipid transition to below −12 °C (to be published). Moreover, a direct proof that the intensity of the methyl band around 2935 cm^{-1} varies with the change in the environment of side-chain methyl and methylene groups of a polypeptide, can be assessed from the Raman spectra of racemic mixtures of poly(γ-benzyl glutamate). Wilser and Fitchen [38] have observed about a 50% change in the intensity of C-H bending vibration (1435 cm^{-1}) in the 50% mixture of left and right enantiomers of poly(γ-benzyl glutamate). It is well known now that changes in the C-H deformation vibrations (1400–1500 cm^{-1} region) influence the intensity and position of C-H stretching (2800–3000 cm^{-1}) vibrations due to Fermi resonance [39]. Taken together, these results suggest that the high temperature transition could involve hydrophobic amino acid residues and lipid chains at apolar protein lipid boundaries. Several other independent physical techniques have also revealed a transition in this temperature range [32,33,40].

In δ-HCCH lysed ghosts, the higher temperature transition monitored by the ratio (I_{2935}/I_{2850}) drastically shifts towards the lower temperature (midpoint about 18 °C). This drastic modification of the thermotropic transition suggests many possibilities. (i) δ-HCCH directly interacts with membrane proteins that may lead to the creation of defects in the secondary or tertiary (folding) structure or to the formation of protein aggregates as created by low pH [35]. Any or all the above defects could in turn influence the orientation of proteins in the membrane and could force the side chains (methyl and methylenes) to differential environment. The latter would be manifested in the intensity changes of the C-H stretching bands [36]. (ii) δ-HCCH disrupts the annulus or 'boundary lipids' [14,18] surrounding transmembrane proteins. This process also could result into the reduction of lipid–protein association and hence could influence protein orientation and dynamics. (iii) Since δ-HCCH was added to live cells, it could have activated some enzymatic process causing chemical modification of proteins. This process would alter the structure of proteins. The first two possibilities can be further evaluated by Raman spectroscopy while the third needs a biochemical support. Parries and Hokin-Neaverson reported that δ-HCCH strongly inhibits the activity of Na^+,K^+-ATPase of human erythrocyte ghosts [14]. It is well known that Na^+,K^+-ATPase regulates cellular volume as well as pH, nerve impulse and muscle contraction [41]. We do not know whether the inhibition of Na^+,K^+-ATPase in intact cells could cause the lysis of erythrocytes. On the other hand our Raman spectroscopic data have provided evidence that δ-HCCH induces changes in the structure of membrane proteins and alters the environment of side chain amino acid residues of cytoskeleton proteins.

Many bands and shoulders other than those associated with the backbone structures of proteins appear in the amide I and III region and their assignment is complicated. We propose that a major contribution to the several overlapping bands in the amide I and III regions is from glutamate, aspartate, NH_3^+ etc. residues of highly amidated segments of the cytoskeleton proteins [42]. This is not surprising since ghost membranes contain a substantial amount of spectrin which is highly amidated like myosin. The high level of glutamate and aspartate amidation is essential to produce visco-elastic properties in wheat proteins [43]. Higher amidation of cytoskeleton proteins of erythrocytes could also be essential and perhaps responsible for maintaining the shape and mechanical properties of red blood cells.

We support the presence of highly amidated segments in ghost cytoskeleton proteins from comparing their Raman features in the 1600 ± 20 cm^{-1} and 1300 cm^{-1} regions with those of authentic amino acids, amidated compounds and relevant polypeptides and proteins. For example α-casein [1342s, 1270sh, 1254s cm^{-1} (44), lysozyme (1338s, 1262s cm^{-1} [45]), myosin (1342s, 1320s, 1304s, 1265s cm^{-1} [44]), and tropomyosin (1342s, 1325s, 1293m, 1253w cm^{-1} [28]), where a major fraction of aspartate and glutamate residues are amidated, show a strong band around 1340 ± 2 cm^{-1} together with the amide III band(s) in this region. Although the 1340 ± 2 cm^{-1} feature has also been assigned to tryptophan [27] in some proteins but a band appears at 1337 cm^{-1} of medium intensity in RNAse [27] which lacks tryptophan. We, therefore, assign this and other bands in the region 1300–1350 cm^{-1} to amidated residues of skeleton proteins (among them the amount of spectrin is higher). These bands are absent in the spectrum of isolated and purified band 3, a major integral erythrocyte protein (Fig. 7, thick line spectrum). Band 3 shows two major bands at 1297 and 1261 cm^{-1}. We assign the 1307 cm^{-1} feature of control erythrocyte ghosts (Fig. 7, thin line spectrum), to α-helix. The position of the helical amide III band depends on the side chains of the amino acids comprising that segment (38). Poly(L-glutamate) yield a strong band at 1307 cm^{-1} and a strong shoulder at 1247 cm^{-1} [28] while in poly(γ-benzyl glutamate) the amide III band appears at 1291 cm^{-1} [38]. On the basis of the above discussion, we suggest that the amidated segments of cytoskeleton proteins yield many overlapping bands in the 1300–1350 cm^{-1} region. We further suggest that the environment of amidated residues is altered in δ-HCCH lysed ghosts.

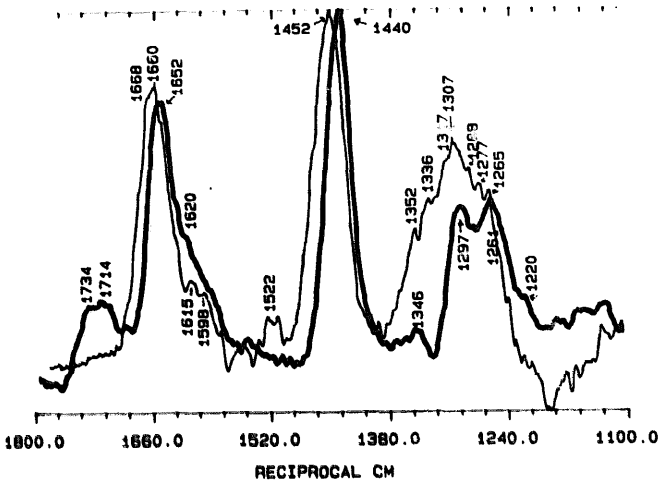

Fig. 7. Raman spectra of Band 3 isolated from control ghosts (prepared by using the method of Okoye, V.C.N. and Bennett, V. (1985) Science 227, 169–171) (thick-line spectrum), showing the 1100–1750 cm^{-1} region. The Raman spectrum of control ghosts (thin-line spectrum) has been shown for the sake of comparison. Spectra recording conditions are same as in Fig. 2. Spectral contributions of water and total lipids have been subtracted as mentioned in Methods.

That erythrocyte proteins contain amidated residues is also suggested by the analysis of the 1600–1620 cm^{-1} region. It is known that ring vibrations of aromatic amino acid residues contribute to the shoulders in the 1600–1620 cm^{-1} region. However, as we have shown in Fig. 6 that asparagine and glutamine [29] also yield a band around 1617 cm^{-1} which splits into 1636 and 1590 cm^{-1} bands of about equal intensity when asparagine is exposed to 0.1 M KCl. The ring vibration of tyrosine, which also appears in this region, does not shift to below 1608 cm^{-1} (base solution). Therefore, the shoulders in the region 1600–1620 cm^{-1} could be assigned to both asparagine and glutamine residues. That the amount of glutamine/asparagine residues is higher than those of tyrosines in erythrocyte proteins [46], further supports our assignment. The spectrum of δ-HCCH lysed ghosts reveals a strong band at 1595 cm^{-1}. The position of this band is closer to the shifted band of asparagine in 0.1 M KCl. Taken together, these data suggests that the highly amidated segments of cytoskeleton proteins are exposed to hydrophilic environment in the δ-HCCH treated erythrocytes. The important question is that how would one relate the above changes in cytoskeleton proteins (spectrin, ankyrin) to the changes observed in the thermal transitions that are probably related to lipids and integral membrane proteins (Band 3 and glycophorin A). There are several lines of evidence that suggest spectrin cytoskeleton is linked to transmembrane proteins [42]. It has also been proposed that spectrin may interact with membrane lipids and stabilize lipid bilayer asymmetry [47]. Considering these models, it is tempting to suggest that the interaction of δ-HCCH with cytoskeleton or with integral proteins could bring massive alterations in the lipid bilayer structure. However, the present data do not distinguish whether the insertion of δ-HCCH into the bilayers brought changes in the membrane proteins or vice versa. These possibilities could be evaluated using the purified spectrin and band 3 reconstituted liposomes where the interaction of δ-HCCH with proteins and lipids can be controlled and the concomitant structural parameters can be evaluated.

It is clear from our studies that the interaction of δ-HCCH with red blood cells have multiple effects. Cell lysis could occur from the insertion of δ-HCCH into lipids that somehow affects cytoskeleton proteins. The detrimental effects that prelysing concentrations of δ-HCCH would exert on red cell shape and mechanical properties will have many pathological implications. Our data may also be significant in view of other cell systems. For example, spectrin is also found in brain homogenates [48] and ghost protein 4.1 has a similarity with neural protein synapsin. Protein 4.1 binds with spectrin in erythrocytes. Synapsin is one of the brain's major substrate for cyclic AMP and Ca^{2+}-calmodulin-dependent kinases and spectrin-synapsin linkage may play a role in neurotransmission. The structural role of spectrin in synaptic vesicles could be parallel to its role in red blood cells. Considering these structural similarities, one may use erythrocytes as a model membrane to explain the pesticidic activities of hexachlorocyclohexane.

Acknowledgements

These studies are supported by US EPA under assistance agreement No. CR-813-481-01-1 to the Center for Environmental Management, Tufts University, Medford, MA. These studies do not reflect the view of EPA and no official endorsement should be inferred. We sincerely thank Dr. Carl F. Blackman, EPA, Research Triangle Park, NC, and Dr. Mark Boyer, Department of Community Health, Tufts University School of Medicine, Boston, MA, for many helpful discussions and advice during this work.

References

1 Hornstein, I. (1955) Science 121, 206–207.
2 Beeman, R.W. (1982) Annu. Rev. Entomol. 27, 253–281.
3 Jones, O.T. and Lee, A.G. (1985) Biochim. Biophys. Acta 812, 731–739.
4 Omann, G. and Lakowicz, J.R. (1982) Biochim. Biophys. Acta 684, 83–95.
5 Damael, A. Lepot, D., Cossarini-Dunier, M. and Monod, G. (1987) Ecotoxicol. Environ. Safety 13, 346–351.
6 Jones, O.T., Froud, R.J. and Lee, A.G. (1985) Biochim. Biophys. Acta 812, 740–751.
7 Bloomquist, J.R., Adams, P.M. and Soderlund, D.M. (1986) Neurotoxicology 7, 11—0.

8 Publicover, S.J. and Duncan, O.J. (1979) Naunyn-Schmicdeberg's Arch. Pharmacol. 308, 179–182.
9 Narahashi, T. and Hass, H.G. (1968) J. Gen. Physiol. 51, 177–198.
10 Beridge, M.J. (1984) Biochem. J. 220, 345–360.
11 Ristow, H.J., Messmer, T.O., Walter, S. and Dieter, P. (1980) J. Cell Physiol. 103, 263–269.
12 Hoffman, R., Erzberger, P., Frank, W. and Rostow, H.J. (1980) Biochim. Biophys. Acta 618, 282–292.
13 Vu, N., Chepko, G. and Zelenka, P. (1983) Biochim. Biophys. Acta 750, 105–111.
14 Parries, G.S. and Hokin-Neaverson, M. (1985) J. Biol. Chem. 260, 2687–2693.
15 Kuhns, D.P., Kaplan, S.S. and Basford, R.E. (1986) Blood 68, 535–540.
16 Omann, G.M. and Lakowicz, J.R. (1982) Biochim. Biophys. Acta 684, 83–95.
17 Antunes-Madeira, M.C. and Madeira, V.M.C. (1989) Biochim. Biophys. Acta 982, 161–166.
18 Verma, S.P. and Rastogi, A. (1990) Biochim. Biophys. Acta 1027, 59–64.
19 Chefurka, W., Chateler, R.C. and Sawyer, W.H. (1987) Biochim. Biophys. Acta 896, 181–186.
20 Stidham, M.A., Siedow, J.N., McIntosh, T.J., Porter, N.A. and Moreland, D.E. (1985) Biochim. Biophys. Acta 812, 721–730.
21 Verma, S.P. and Sonwalkar, N. (1991) Radiat. Res. 126, 27–35.
22 Williams, R.W., McIntyre, J.O., Gaber, B.P. and Fleischer, S. (1986) J. Biol. Chem. 261, 14520–14524.
23 Verma, S.P. and Wallach, D.F.H. (1983) in Membrane Structure and Function (Chapman, D., ed.), pp. 167–192, Macmillan Press, London.
24 Verma, S.P., Philippot, J.R., Bonnet, B., Sainte-Marie, J., Moschetto, Y. and Wallach, D.F.H. (1985) Lipids 20, 890–896.
25 Lippert, J.L., Gorezyca, L.E. and Meiklejohn, G. (1975) Biochim. Biophys. Acta 382, 51–56.
26 Wallach, D.F.H. and Verma, S.P. (1975) Biochim. Biophys. Acta 382, 542–551.
27 Tu, A.T. (1982) Raman spectroscopy in Biology: Principles and Applications, pp. 65–116, John Wiley and Sons, New York.
28 Koenig, J.L. (1972) J. Polymer Sci. Part D 59–177.
29 Schmidt-Ullrich, R., Verma, S.P. and Wallach, D.F.H. (1976) Biochim. Biophys. Acta 426, 477–488.
30 Dolish, F.R. Fateley, W.G. and Bentley, F.F. (1974) Characteristic Raman Frequencies of Organic Compounds, pp. 124–125, John Wiley and Sons, New York.
31 Verma, S.P. and Wallach, D.F.H. (1976) Proc. Natl. Acad. Sci. USA 73, 3358–3561.
32 Sato, B.K., Nishikida, K., Samuels, I. and Tyler, F. (1978) J. Clin. Invest. 61, 251–257.
33 Nigg, E.A. and Cherry, R.J. (1979) Biochemistry 18, 3457–3465.
34 Mikkelsen, R.B., Verma, S.P. and Wallach, D.F.H. (1978) Proc. Natl. Acad. Sci. USA 75, 5478–5482.
35 Pinto da Silva, P. (1972) J. Cell Biol. 53, 777–787.
36 Verma, S.P and Wallach, D.F.H. (1977) Biochem. Biophys. Res. Commun. 74, 473–479.
37 Brands, J.F. and Hunt, L. (1967) J. Am. Chem. Soc. 89, 4826–4838.
38 Wilser, W.T. and Fitchen, D.B. (1974) Biopolymers 13, 1435–1445.
39 Schachtschneider, I. and Snyder, F. (1963) Spectrochim. Acta 19, 117–168.
40 Bieri, V. and Wallach, D.F.H. (1975) Biochim. Biophys. Acta 406, 415–423.
41 Skou, J.C. (1988) Methods Enzymol. 156, 1–25.
42 Bennet, V. (1982) J. Cellul. Biol. 18, 46–95.
43 Beckwith, A.C., Wall, J.S. and Dimler, R.J. (1963) Arch. Biochem. Biophys. 103, 319–330.
44 Frushour, B.G. and Koenig, J.L. (1974) Biopolymers 13, 1809–1819.
45 Lord, R.C. and Yu, N.T. (1970) J. Mol. Biol. 50, 509–524.
46 Rosenberg, S.A. and Guidotti, G. (1968) J. Biol. Chem. 243, 1985–1992.
47 Mombers, C., Verkleij, A.J., De Gier, J. and Van Deenen, L.L.M. (1979) Biochim. Biophys. Acta 551, 271–281.
48 Baines, A.J. and Bennett, V. (1985) Nature 315, 410–413.